Multistability and Memory Effect in a Highly Turbulent Flow: Experimental Evidence for a Global Bifurcation

Florent Ravelet, Louis Marié, Arnaud Chiffaudel,* and François Daviaud
Service de Physique de l'État Condensé, DSM, CEA Saclay, CNRS URA 2464, 91191 Gif-sur-Yvette, France
(Received 19 May 2004; published 15 October 2004)

We report experimental evidence of a global bifurcation on a highly turbulent von Kármán flow. The mean flow presents multiple solutions: the canonical symmetric solution becomes marginally unstable towards a flow which breaks the basic symmetry of the driving apparatus even at very large Reynolds numbers. The global bifurcation between these states is highly subcritical and the system thus keeps a memory of its history. The transition recalls low-dimension dynamical system transitions and exhibits very peculiar statistics. We discuss the role of turbulence in two ways: the multiplicity of hydrodynamical solutions and the effect of fluctuations on the nature of transitions.

DOI: 10.1103/PhysRevLett.93.164501 PACS numbers: 47.20.Ky, 05.45.–a, 47.20.Ft, 47.27.Sd

Nonlinear systems generally present multiple solutions and various transitions between them. Moreover, stability and transitions are influenced by the presence of noise and/or fluctuations. In the field of turbulence, the question of multistability of turbulent flows, for example, in tornadoes [1,2], delta-wing flow [3], wakes [4], and vortex breakdown [5], remains open and unsolved. While multiple analytical or numerical solutions are often encountered for the Navier-Stokes equation at even moderate Reynolds number (e.g., for swirling flows [2,5–8]), these solutions are generally neither experimentally relevant, nor stable at very high Reynolds number. Furthermore, turbulent flows at very high Reynolds number are generally expected to statistically respect the basic symmetries of their driving apparatus. Indeed, even if bifurcations and symmetry breaks occur on the way to turbulence, the fully developed turbulent state is known to restore the broken symmetries, in the limit of infinite Reynolds number and far from boundaries [9]. In this Letter, we experimentally study the multistability of a turbulent von Kármán flow between two counterrotating disks in a finite vessel at very high Reynolds number. This system undergoes a subcritical global bifurcation between turbulent states characterized by mean flows of different topology and symmetry. These turbulent states coexist at high Reynolds number and can be "prepared" specifically; i.e., they keep a memory of the system history. Since these states are highly fluctuating turbulent states, we also address the question of the role of the fluctuations for such a transition. Actually, the effect of an external noise on an existing transition is well documented [10], but the global bifurcation reported here does take place only over an already fluctuating turbulent regime. Does fluctuation trigger the bifurcation as multiplicative noise does for nonlinear oscillators [11] and turbulent α effect does for dynamo action [12]?

Experimental setup.—We call von Kármán-type flow the flow generated between two coaxial counterrotating impellers in a cylindrical vessel. The cylinder radius and height are, respectively, $R = 100$ mm and $H_c = 500$ mm. We use bladed disks to ensure inertial stirring. Most of the inertially driven von Kármán setups studied in the past dealt with straight blades [13,14]. In this Letter, the impellers consist of 185 mm diameter disks each fitted with 16 curved blades: curvature radius 50 mm, height 20 mm (Fig. 1). The distance between the inner faces of the disks is $H = 180$ mm, which defines a working space for the flow of aspect ratio $H/R = 1.8$. With curved blades, the directions of rotation are no longer equivalent. We rotate the impellers clockwise (with the concave face of the blades). Four baffles ($10 \times 10 \times 125$ mm) can be added along the cylinder wall.

The impellers are driven by two independent brushless 1.8 kW motors, with speed servo loop control. The motor rotation frequencies f_1, f_2 can be varied independently in the range 0–15 Hz. An experiment is thus characterized by two numbers: $f = \sqrt{(f_1^2 + f_2^2)/2}$ measuring the intensity of the forcing and $\theta = (f_2 - f_1)/(f_1 + f_2)$ measuring the speed dissymmetry ($-1 \leq \theta \leq 1$). For exact counterrotation, $f_1 = f_2 = f$ and $\theta = 0$. The speed servo loop control ensures a precision of 0.5% on f, and an absolute precision of ± 0.002 on θ for small values.

The working fluid is water, thermoregulated within ± 1 K. Velocity fields are measured by laser doppler velocimetry (LDV). Torques are measured as an image of the current consumption in the motors given by the servo drives and have been calibrated by calorimetry. For a typical frequency $f = 4$ Hz at 35 °C, the integral Reynolds number is $\mathrm{Re} = 2\pi f R^2 \nu^{-1} \simeq 3 \times 10^5$ and the

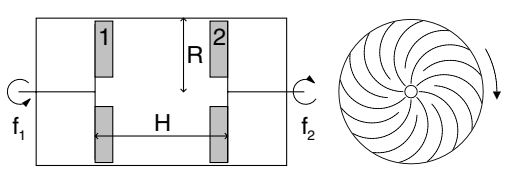

FIG. 1. Sketch of the experimental setup and of the impellers blade profile. The arrow indicates the positive rotation sense.

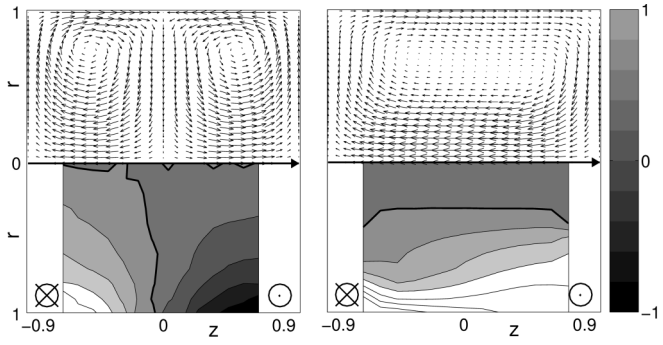

FIG. 2. Dimensionless mean velocity field measured at $\theta = 0$ by LDV over 120 integral turnover times by grid point to ensure good convergence; $f = 2$ Hz ($\mathrm{Re} = 1.5 \times 10^5$). Left: symmetric state (s). Right: bifurcated state (b_1). Space coordinates in units of R. Gray code stands for azimuthal velocity. Isolines are distant of 0.2 and the gray code saturates in the right map. Bold lines indicate level zero.

velocity fluctuation level is of order 30%: the flow is highly turbulent.

The von Kármán flow phenomenology is the following. Each impeller acts as a centrifugal pump: the fluid rotates with the impeller and is expelled radially. It is pumped in the center of the impeller. In the exact counterrotating regime, the flow is divided into two toric cells separated by an azimuthal shear layer. The problem (equation and boundary conditions) is invariant under rotations of π ($\mathcal{R}_\pi$) around any radial axis passing through the center of the cylinder. The velocity field is expected to be $\mathcal{R}_\pi$ invariant.

A "statistical" symmetry breaking.—In our high Reynolds number regime, the flow is highly turbulent. For instance the rms value of the velocity is of the same order of magnitude as the mean value. In Fig. 2 (left), we present a map of the mean part of the exact counterrotation flow measured by LDV. Two cells are observed, and the flow is $\mathcal{R}_\pi$ invariant: the symmetries are statistically restored [9]. The mean angular momentum of the fluid is equal to zero: the two impellers produce the same mean torque to maintain the flow. This situation is well known and documented. We label this symmetric state (s).

However, with our curved blades, we observe for small θ a global bifurcation of the flow after a certain time t_{bif}: both mean velocity field and torques display dramatic changes (Fig. 3). The two torques are suddenly 4 times larger and are no longer equal. The mean flow exhibits only one cell (Fig. 2, right). In the bulk, the fluid is pumped toward impeller 1 without rotation. Then the fluid is expelled radially and starts spiraling along the cylinder until it meets impeller 2, which rotates in the opposite direction. It is abruptly stopped and reinjected near the axis. We label this state (b_1). A third state (b_2) is deduced from (b_1) by exchanging the roles of impellers 1 and 2. In bifurcated states(b_1) or (b_2), the fluid is globally in rotation: the mean angular momentum is not zero.

Finally, three states are observed: the canonical $\mathcal{R}_\pi$ invariant (in a statistical sense) state (s) and two

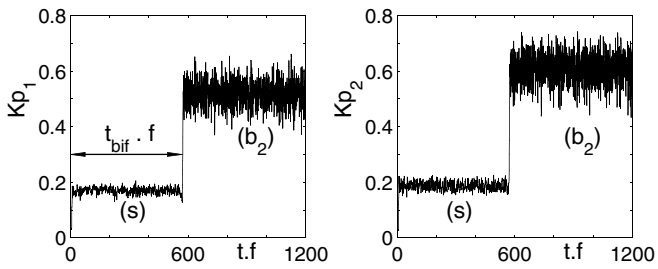

FIG. 3. Time series of dimensionless torque showing the bifurcation $(s) \rightarrow (b_2)$, for $\theta = 0.0204$, $f = 4.08$ Hz. Left: torque on impeller 1. Right: torque on impeller 2. The bifurcation time is the time when the torque on impeller 1 reaches 140% of the mean value for the symmetric state (s).

bifurcated states which break the $\mathcal{R}_\pi$ symmetry at $\theta = 0$ but are the images one of the other by $\mathcal{R}_\pi$. We detail in the next section the transitions between these different states.

Hysteresis loops.—The difference between the two torques characterizes the different states. We have checked that, as expected for so high a Reynolds number [9], the torque T given by one impeller for a given (f, θ) does not depend on Re and scales as $T(f, \theta) = K_p(\theta)\rho R^5(2\pi f)^2$ [14], with ρ the fluid density and K_p a dimensionless power coefficient.

In Fig. 4, we plot the dimensionless difference ΔK_p between the two torques versus θ for several configurations. For straight blades, we observe a continuous curve from $\theta = -1$ to $\theta = 1$ [Fig. 4(a)] with two transitions between one- and two-cell flows at $\theta = \pm 0.13$. For impellers with curved blades and no baffles on the cylinder wall, we observe the three states in Fig. 4(b). For $\theta = 0$, we recognize state (s) ($\Delta K_p = 0$) and both bifurcated states (b_1) and (b_2). The state (s) branch is almost reduced to one point and can be reached only by starting the two

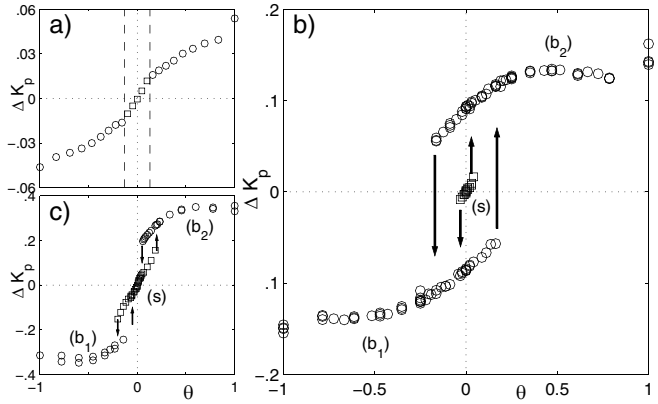

FIG. 4. Dimensionless torque difference ΔK_p versus θ for Re in the range 2–8×10^5. Straight blades (a) exhibit continuous transition from one-cell flow to two-cells flow for $\theta = \pm 0.13$ (vertical lines). Curved blades without (b) or with (c) baffles along cylinder wall show subcritical transitions between symmetric/two-cell (s), (□), and bifurcated/one-cell (b_1), (b_2) states (○).

motors simultaneously. Its stability is discussed in the next section. The bifurcated state (b_1) lies on a branch coming continuously from $\theta = -1$ $(f_2 = 0)$. Starting from $\theta = -1$ and increasing θ, we stay on the (b_1) branch even for $\theta > 0$: impeller 1 keeps rotating and pumping the fluid although its rotation rate is weaker than the impeller 2 rotation rate. For $\theta \simeq 0.16$, there is a transition from (b_1) to (b_2): the fluid abruptly changes its sense of rotation. There is a large hysteretic cycle. Note that it is impossible to reach the symmetric state (s) this way. The global quantities of this highly turbulent flow keep memory of the way the system has been started from rest. An intermediate situation is reached with the same curved blades and baffles on the wall [Fig. 4(c)]. Baffles break the spiraling flow along the wall of the cylinder, which is a major feature of the bifurcated state velocity field. The hysteretic cycle splits into two classical first-order cycles: the central symmetric state becomes stable and can be obtained from any initial condition.

Stability of the central branch (s).—We focus now on the transition from symmetric state to bifurcated state for curved blades without baffles. As mentioned before, the central branch is very small and, for a given (f, θ), the transition occurs after a certain time t_{bif} which exhibits a complex statistics.

So we performed the following experiments: starting from rest, we simultaneously start both motors to a given (f, θ) with a short ramp (typically 1 s) and record the torques. A few seconds after the instant t_{bif} when bifurcation occurs, we stop the motors, wait a minute, and run again. We perform typically 500 runs to get the distribution of bifurcation times. The cumulative distribution function (CDF) for t_{bif} (Fig. 5) shows exponential behavior for the probability of staying in the symmetric state a time greater than t: $P(t_{bif} > t) = A \exp[-(t - t_0)/\tau]$, where t_0 is characteristic of the transition duration $(t_0 f \sim 5)$. Thus, we obtain a characteristic bifurcation time $\tau(f, \theta)$ by a nonlinear fitting of the CDF. We performed the experiment for three values of f. The results are shown in Fig. 6 in a log-log scale. There is no noticeable dependence on f and τ behaves as $|\theta|^{-6}$. So, as θ tends to zero, τ diverges very fast to infinity: the central point is marginally stable. The physical phenomenon at the origin of such an exponent remains to be understood.

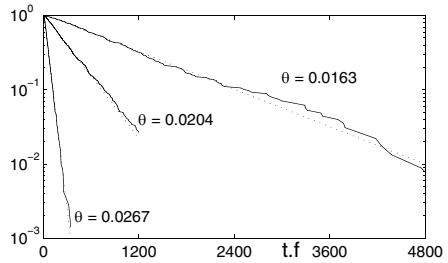

FIG. 5. Cumulative density function of bifurcation times for three different θ at $f = 4.16$ Hz. Dotted lines: nonlinear exponential fits.

Discussion.—The experiment presented here brings mainly two issues: (i) the existence and the nature of multiple regimes for this turbulent flow, and (ii) the role of the noise or the fluctuations in some transitions between these flow regimes, i.e., the stability problem for the two-cell (s) branch.

We first try to explain the existence of multiple stable regimes by hydrodynamical basic arguments. The von Kármán (VK) class of Navier-Stokes solutions in semi-infinite space with one or two infinite rotating disks for end conditions has been extensively studied since 1921 [6,7,15]. Experiments are necessarily limited in diameter and do not strictly belong to the same class. However, the approximation is very commonly made, at least for small H/R. In practice, in our system, and in the spirit of Batchelor [6] and Stewartson [7], we construct finite-aspect-ratio solutions of our experimental VK problem at high Re (Fig. 2) with (i) any typical truncated Batchelor [6] solution for $0 \leq r \lesssim R/2$, together with (ii) some recirculation flow in rotation in $R/2 \lesssim r \lesssim R$ and (iii) a thin boundary layer near the outer cylinder which matches this rotation [16]. The two-cell mean flow (s) is simply described in the laboratory frame by two rotating regions inertially driven by the blades and separated by a shear layer near midheight. Both disks centrifugally expel the fluid. Let us now consider one-cell flows (b_1) and (b_2). Since one disk expels the fluid and the other reinjects it to the center, these flows resemble the corotating $(f_1 f_2 < 0)$ regime solutions [6,7] characterized by uniform rotation of the bulk, a boundary layer on each disk, pumping from one disk to the other, and recirculation at infinity. This solution has no shear layer. We note that mean bulk rotation, for $r \lesssim R/2$, is close to zero (Fig. 2, right). In conclusion, we can make the assumption that flows (b_1) and (b_2) are equivalent to corotating flows observed in two oppositely rotating frames of frequencies $+f_r$ and $-f_r$, with $|f_r| > \max(|f_1|, |f_2|)$. This is consistent with the fact that the single cell flows (b_1) and (b_2) exhibit global rotation in the outer shell $R/2 \lesssim r \lesssim R$. The stability of such a solution is clearly enhanced by the concave curved blades that enforce rotation of the fluid near the outer cylinder.

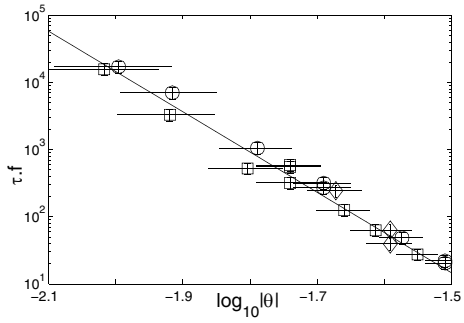

FIG. 6. τf versus θ for $f = 4.16$ Hz/Re $= 3.3 \times 10^5$ (○), $f = 6$ Hz/Re $= 4.7 \times 10^5$ (□), and $f = 10$ Hz/Re $= 7.9 \times 10^5$ (◇), fitted by a -6 slope power law.

We can now consider how these three solution branches exchange their stability. First, note that the bifurcation diagrams respect the $\mathcal{R}_\pi$ symmetry: $\theta \to -\theta; \Delta K_p \to -\Delta K_p$. The straight-blade diagram [Fig. 4(a)] is continuous: from left to right two second-order transitions $(b_1) \leftrightarrow (s)$ and $(s) \leftrightarrow (b_2)$ are observed as in small H/R systems [17]. On the contrary, the curved blade diagram [Fig. 4(b)] is strongly hysteretic. The addition of baffles [Fig. 4(c)] allows one to remove a degeneracy: baffles drag disturb the outer cylinder boundary layer flow, thus lowering the relative stability of one-cell flows with respect to the two-cell flow. The large hysteresis cycle is split into two classical first-order bifurcations. This singular cycle can thus be viewed as the result of the collapse or collision of two first-order cycles. Similar cycles are encountered in conical [18] and delta-wing flows [3]. The memory effect—if the system is currently on (s), both driving frequencies *must* have been increased in parallel—is thus essentially a consequence of the cycle structure.

In order to test the effect of turbulence on the stability of the observed flows, we lowered the Reynolds number down to laminar using water/glycerol mixtures. While $\mathrm{Re} \lesssim 1000$, no multiplicity is observed: the bifurcation diagram is similar to the straight-blade diagram of Fig. 4(a). The cycle appears for Re between 1000 and 3000. The study is in progress and will be reported elsewhere. The high Reynolds behavior reported in this Letter is well established once $\mathrm{Re} \gtrsim 5000$. Thus, multiplicity appears with turbulence but does not with laminar ($\mathrm{Re} \lesssim 110$) nor chaotic ($\mathrm{Re} \lesssim 1000$) flows. A possible explanation for the multiplicity could thus be the evolution of the outer cylinder boundary layer with Re.

Besides, the statistical nature of the transitions themselves is probably related to turbulent fluctuations. Let us first notice that the bifurcation studied here corresponds to exchange of stability between mean flows, these mean states never being realized at any given time. Is the bifurcation formalism exactly valid for our mean flows? In some aspects, our system behaves as a low-dimension dynamical system, as in the turbulent spiral transition observed in wide-aspect-ratio Taylor-Couette flow [19] or in the noise-induced Hopf bifurcation for a Duffing oscillator with multiplicative white noise [11]. However, if a nonlinear amplitude equation could correctly describe the shape bifurcation diagram, it would probably not be able to catch the statistics of the transition from the two-cell state (s) to a one-cell state (b_1) or (b_2). This transition shows very peculiar statistics, with a very high critical exponent -6 (Fig. 6). It also strictly respects a forbidden-transition rule: the horizontal axis of the bifurcation diagram is never crossed; i.e., $(s) \to (b_2)$ [respectively, $(s) \to (b_1)$] is forbidden for $\theta < 0$ [respectively, $\theta > 0$]. This observational fact could by itself justify the stability of the central point $\theta = 0$, which has to respect both rules. Furthermore, the noncrossing of the axis could be the signature of multiplicative noise as suggested to account for small-scale turbulence [20].

The global bifurcation reported in this Letter presents a very unusual bifurcation diagram. Some features about the multistability have been searched among the mechanics of high-Reynolds-number flows, while some others simply involve the theory of nonlinear bifurcations, possibly in the presence of noise. Among the transitions, the two-cell $\to$ one-cell stability exchange plays a remarkable role in presenting original statistics of transition and putting the flow definitively in a state which breaks the $\mathcal{R}_\pi$ symmetry of the system and does not allow the flow to restore statistically this symmetry when $\mathrm{Re} \to \infty$.

We thank V. Padilla and C. Gasquet for their efficient assistance in building and piloting the experiment, and B. Dubrulle, O. Dauchot, and N. Leprovost for fruitful discussions.

*Electronic address: arnaud.chiffaudel@cea.fr

[1] O. R. Burrgraf and M. R. Foster, J. Fluid Mech. **80**, 685 (1977).
[2] V. Shtern and F. Hussain, Phys. Fluids A **5**, 2183 (1993).
[3] M. G. Goman, S. B. Zakharov, and A. N. Khrabrov, Sov. Phys. Dokl. **30**, 323 (1985).
[4] G. Schewe, J. Fluid Mech. **133**, 265 (1983).
[5] V. Shtern and F. Hussain, Annu. Rev. Fluid Mech. **31**, 537 (1999).
[6] G. K. Batchelor, Q. J. Mech. Appl. Math. **4**, 29 (1951).
[7] K. Stewartson, Proc. Cambridge Philos. Soc. **49**, 333 (1953).
[8] P. J. Zandbergen and G. Dijkstra, Annu. Rev. Fluid Mech. **19**, 465 (1987).
[9] U. Frisch, *Turbulence—The Legacy of A. N. Kolmogorov* (Cambridge University Press, New York, 1995).
[10] S. Residori *et al.*, Phys. Rev. Lett. **88**, 024502 (2002).
[11] K. Mallick and P. Marcq, Eur. Phys. J. B **31**, 553 (2003); Eur. Phys. J. B **36**, 119 (2003).
[12] H. K. Moffatt, *Magnetic Field Generation in Elecrically Conducting Fluids* (Cambridge University Press, Cambridge, 1978).
[13] O. Cadot, S. Douady, and Y. Couder, Phys. Fluids **7**, 630 (1995).
[14] R. Labbé, J. F. Pinton, and S. Fauve, J. Phys. II (France) **6**, 1099 (1996).
[15] T. von Kármán, Z. Angew. Math. Mech. **1**, 233 (1921).
[16] We have experimentally shown (L. Marié, Ph.D. thesis, University Paris 7, 2003) that, when using inertial stirring bladed disks at high Reynolds number, the flat outer rotating cylinder may be rotated almost without any effect but develops a thin viscous boundary layer on it. The torque exerted through this layer can generally be neglected with respect to the impeller torques.
[17] G. Dijkstra and G. J. F. van Heijst, J. Fluid Mech. **128**, 123 (1983).
[18] V. Shtern and F. Hussain, J. Fluid Mech. **309**, 1 (1996).
[19] A. Prigent *et al.*, Phys. Rev. Lett. **89**, 014501 (2002).
[20] J.-P. Laval, B. Dubrulle, and S. Nazarenko, Phys. Fluids **13**, 1995 (2001).